Nodal Sensitivity-Based Smart Inverter Control for Voltage Regulation in Distribution Feeder

Oğuzhan Ceylan, *Member, IEEE*, Sumit Paudyal, *Member, IEEE,* and Ioana Pisica, *Senior Member, IEEE*

Abstract—Over-voltage is one of the issues in distribution grids with high penetration of photovoltaics (PVs). Centralized or droop-based methods of active power curtailment (APC) and/or reactive power control of PVs are viable solutions to prevent over-voltage. This paper proposes two distributed methods to control PV inverters which are based on nodal sensitivities. Then, the performance of the proposed methods is compared with two commonly used control methods, i.e., a distributed method that follows IEEE-1547 but uses arbitrarily chosen droops and a centralized optimal power flow (OPF)-based method. Performance is evaluated using a 730-node feeder with up to 100% penetration of inverters. Based on the case studies, the key findings are: *a)* local droop setting as per IEEE-1547, whether the droops are arbitrarily chosen or systematically calculated using sensitivities, can eliminate over-voltage if reactive power control and APC are coordinated, *b)* the proposed sensitivity-based approach yields the best voltage performance index computed based on voltage profile compared to the maximum allowed upper bound, and *c)* OPF-based method is desirable if communication infrastructure exists and minimum energy curtailment is sought.

Index Terms—Photovoltaic, distribution grid, over-voltage, smart inverter, voltage control, optimal power flow.

I. Nomenclature

α	Percentage of maximum reactive power capability.
β, γ	Slope of droop curves.
Δt	Time interval.
ΔV	Voltage change on a node.
ΔV^{Rq}	Required voltage change.
$\frac{\delta \Theta}{\delta P}, \frac{\delta \Theta}{\delta Q}, \frac{\delta V}{\delta P}, \frac{\delta V}{\delta Q}$	Sensitivities.
Θ	Voltage angle.
ω	Window of time.
e	End node of a lateral.
E^{cur}	Curtailed energy.
I	Nodal current injection.
j, k	Set of nodes, $j, k \in \{1, 2, .., N\}$.
l	Set of laterals, $l \in \{1, 2, 3, .., L\}$.
m, n	Set of nodes with PVs, $m, n \in \{1, 2, 3, .., M\}$.
P^{cur}	Active power curtailment of PVs.
P^L	Active power of load.
P	Available PV generation.
Q^c	Unused reactive power capability of PVs.
Q^{max}	Maximum reactive power capability of PVs.
Q	Reactive power output of PVs.
Q^L	Reactive power of load.

r	Sorted reactive power capability, $r \in \{1, 2, 3, .., R\}$.
$\mathcal{S}$	Sensitivity matrix.
S	Inverter rating.
t	Time index, $t \in \{1, 2, 3, .., T\}$.
V	Nodal voltage.
V^a, V^b, V^c, V^d	Voltage break points.
V^L/V^U	Voltage lower/upper limits for inverter operation.
V^{min}/V^{max}	Voltage lower/upper limits for feeder operation.
Y	Y-bus matrix.

II. Introduction

SOLAR photovoltaic (PV) systems are the fastest growing source of renewable energy being integrated to power grids [1]. This has obvious advantages including economic benefits and less emissions. However, high penetration of rooftop PVs raises a number of concerns to the system operators. High PV penetration causes several operational challenges to the distribution grids including over-voltage [2] and power quality [3]. During high PV generation and low load periods, there could be reverse power flow that leads to voltage rise on the low voltage (LV) feeders [4]. Over-voltage is one of the main reasons for limiting the capacity of PV that can be connected to LV systems [5]. A utility study showed that hosting capacity of LV feeder is limited by over-voltage during an extreme condition of lowest load and maximum PV generation [6].

Conventionally, volt/var regulation on distribution grids is achieved through control of legacy grid devices such as load tap changers and switched capacitors [7], which can now be achieved through the control of smart inverters. In future distribution grids, novel grid applications can be achieved through the coordination of smart inverters [8]. For example, smart inverters can modulate active power (Watt) and reactive power (VAr) injections necessary for system-wide volt/var support. Reactive power support from smart inverters also helps to accommodate higher penetration of distributed PVs without need of system upgrade to some extent [9]. IEEE-1547 requires smart inverters to be capable of consuming or producing reactive power when inverters are at or above 5% of their rated active power [10]. Though active power curtailment (APC) of PVs is more effective on managing distribution grid voltage due to high R/X ratio of feeders [4], [11], the reactive power control should also be considered to reduce unnecessary energy curtailment resulting from the APC based approach alone.

Current literature on prevention of over-voltage in distribution systems with PVs is mainly divided into

centralized and distributed methods for APC and reactive power distpatch. The centralized approaches solve optimal power flow (OPF) or its variants to find the dispatch of active and/or reactive power from the PVs. The centralized approaches demand communication infrastructure, while local approaches are droop-based and avoid the need of communication.

Lin, *et al.*, [12] used a droop-based (**kW/V**) approach for active power (**P**) curtailment. Ghosh, *et al.*, in [13] proposed a droop-based **P** curtailment and reactive power (**Q**) absorption method for controlling the PV inverters. Similarly, Molina-García, *et al.*, proposed piece-wise linear droops to control the voltage with PVs [14]. Mokhtari, *et al.*, in [15] used droop based approach for APC, and empirical **Q(P)** rules to absorb reactive power. Gagrica, *et al.*, in [16] used $\delta V/\delta P$ sensitivities for droop settings. Ku, *et al.*, in [17] used both $\delta V/\delta P$ and $\delta V/\delta Q$ sensitivities to coordinate reactive power absorption and APC of PVs. Demirok, *et al.*, also used $\delta V/\delta P$ and $\delta V/\delta Q$ sensitivities to devise two droop control functions **cosΦ(P)** and **Q(V)** [18]. In [19], reactive power of distributed generators are dispatched based on approximate sensitivities.

The key challenge with the aforementioned local droop-based control techniques is the lack of coordinated operation, which results in non-optimal APC. Moreover, these droop control methods also require to compute threshold power or voltage beyond which the droop becomes effective. However, the inverter operating characteristics curves **Q(V)**, **Q(P)** and **P(Q)**, as defined in the IEEE-1547 [10] are also based on local measurements, and the droops used in the studies [12]–[18] can certainly serve as a basis for the smart inverter settings as per the IEEE-1547.

One of the solutions to address the coordination challenges of decentralized control is to implement centralized control scheme. Weckx, *et al.*, in [20] proposed a centralized optimization-based method that would compute piece-wise linear control function **Q(P)** to use at local controllers for locally adjusting the reactive power. Su, *et al.*, proposed an OPF based approach to find **(P,Q)** set points of the PV inverters in [21]. Zhao, *et al.*, also used OPF based formulation with adaptive weight on objective function to ensure fair curtailment [22]. Cavraro, *et al.*, in [23] demonstrated the value of communication for regulating voltage with PVs by showing instances where local measurement based control approaches (like in [24]) lead to infeasibility issues. Some recent works use combination of centralized and distributed approaches. Ferreira, *et al.*, proposed sensitivity-based ($\delta V/\delta P$) linear centralized optimization approach and a local control methods for finding optimal PV curtailment [25]. Olivier, *et al.*, in [26] proposed distributed control for managing reactive power and curtailing active power systematically. Though a centralized method requires communication, since the IEEE-1547 requires all smart inverters be equipped with communication capability, a centralized OPF based approach for inverter dispatch could be feasible in future distribution grids. Moreover, the obvious advantages of centralized OPF (e.g., less APC [11], fair APC [22]) over distributed control will certainly be a reason for its adoption in future distribution grid management systems.

Since the centralized and distributed methods both for controlling PVs are gaining research attention, and both methods have advantages and shortcomings, in this work we try to examine the performance of both approaches. In this context, the contributions of this work are as following:

- It proposes two distributed methods to regulate voltage in PV-rich distribution networks. The first proposed method uses a sensitivity-based approach, different from the existing approaches such as the one in [19], that includes APC in coordination with reactive power control for voltage control in distribution networks. The second proposed method combines sensitivities with the IEEE-1547 recommended piece-wise droop settings.
- Comparative analyses of the proposed methods are carried out using arbitrary droop settings of **Q(V)** and an OPF-based method. Monte Carlo analyses are also carried out with different PV penetration levels to examine the robustness of the proposed methods.

The rest of the paper is organized as follows: Section III details the local and centralized control methods used on this work; Section IV describes the MV/LV feeder used for the simulation and case studies; and the main conclusions drawn from the paper are provided in Section V.

III. LOCAL AND CENTRALIZED METHODS OF INVERTER CONTROL

A. Reactive Power Control Rules as per IEEE-1547

IEEE-1547 prescribes a set of droops for active and reactive power control based on local voltage at inverter node [10]. Fig. 1 shows an example **Q(V)** droop curve. $\mathbf{V^L}$ and $\mathbf{V^U}$ represent lower and upper limits for the inverter operation, respectively. $\mathbf{V^a}$, $\mathbf{V^b}$, $\mathbf{V^c}$, and $\mathbf{V^d}$ correspond to the voltage break points that define the piece-wise droop settings. IEEE-1547 provides ranges for setting the break points on the **Q(V)** and other droop curves [10]. Fig. 2 shows a schematic diagram of how control rules based on the IEEE-1547 can be implemented. It should be noted that **Q(V)** droop settings can be dispatched on regular intervals from the control center or configured locally.
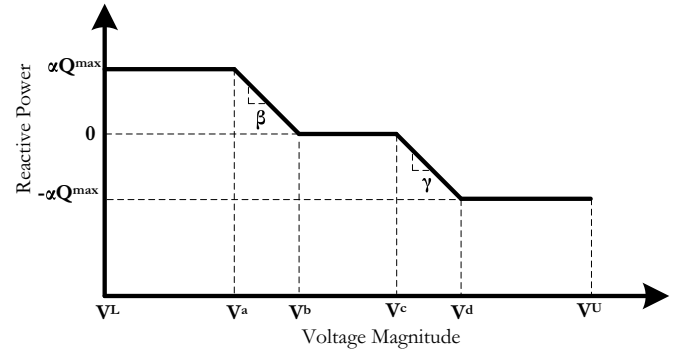

Fig. 1. An example **Q(V)** curve as per IEEE-1547 [10].

Each inverter may use different **Q(V)** droop settings. Each inverter controller checks its local voltage magnitude and if it is smaller than $\mathbf{V^a_m}$, then the inverter injects $\alpha \mathbf{Q^{max}_m}$, i.e., the maximum allowed reactive power injection as percentage of
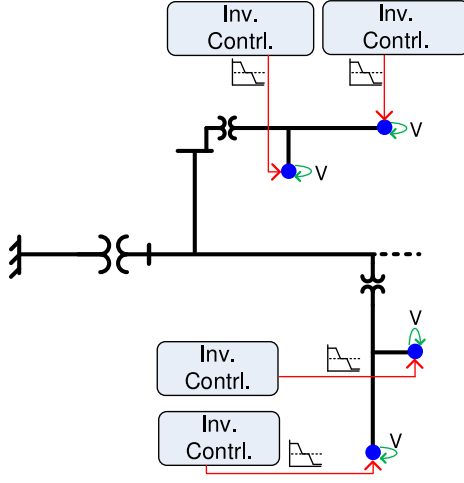
Fig. 2. Active and reactive power control based on IEEE-1547 rules.

total reactive power capability of the inverter. If the voltage magnitude is higher than V_m^d, then the output of inverter is set to $-\alpha Q_m^{max}$. When the measured voltage is within V_m^a and V_m^b, reactive power injection follows the slope β_m. Similarly, when the measured voltage is between V_m^b and V_m^c, then the reactive power output of the inverter follows the slope γ_m. If the measured voltage is between V_m^c and V_m^d, then the reactive power output of the inverter becomes zero. In reactive power priority mode, curtailment of active power may become necessary. To check whether active power curtailment is required or not, $P_m^2 + Q_m^2$ is compared to squared of the inverter's apparent power rating S_m^2. If the latter is smaller, then active power is curtailed. The algorithm of reactive power control and active power curtailment based on the IEEE-1547 prescribed droop settings are given in Algorithm 1.

B. Proposed Approach: Power-flow Sensitivity-based Method

A schematic of inverter control based on proposed sensitivity-based approach is shown in Fig. 3. In the proposed approach, controller works at each lateral level, and using power flow sensitivities computed offline, and based on available real-time nodal voltage measurements, active and reactive power of PVs are dispatched in real time. The power flow sensitivity matrix can be defined as [4],

$$
\mathcal{S} = \begin{bmatrix} \frac{\delta\Theta}{\delta P} & \frac{\delta\Theta}{\delta Q} \\[2mm] \frac{\delta V}{\delta P} & \frac{\delta V}{\delta Q} \end{bmatrix} \tag{1}
$$

For reactive power based voltage control, $\frac{\delta V}{\delta Q}$ are used, while for APC, $\frac{\delta V}{\delta P}$ are used. The coordination among multiple inverters for APC and reactive power control is achieved in the following, and further details are provided in Algorithm 2. The proposed sensitivity based approach checks the voltage magnitudes at the end nodes of each lateral and takes the following control actions,

- If the voltage magnitude of the end node of a lateral is within V_m^a/V_m^d, no new control action is required.

Algorithm 1: Control as per IEEE-1547 Droops

$$\beta_m = \frac{\alpha Q_m^{max}}{V_m^b - V_m^a}$$

$$\gamma_m = \frac{-\alpha Q_m^{max}}{V_m^d - V_m^c}$$

while $t < T$ **do**
  Run Power Flow
  while $m < M$ **do**
    if $V_{m,t} < V_m^a$ **then**
      $Q_{m,t} = \alpha Q_m^{max}$
    else if $V_{m,t} > V_m^d$ **then**
      $Q_{m,t} = -\alpha Q_m^{max}$
    else if $V_{m,t} > V_m^a$ **and** $V_{m,t} < V_m^b$ **then**
      $Q_{m,t} = \alpha Q_m^{max} - \beta_m (V_{m,t} - V_m^a)$
    else
      $Q_{m,t} = -\alpha Q_m^{max} - \gamma_m (V_m^d - V_{m,t})$
    end
    if $Q_{m,t}^2 + P_{m,t}^2 > S_m^2$ **then**
      $P_{m,t}^{cur} = P_{m,t} - \sqrt{S_m^2 - Q_{m,t}^2}$
    end
  end
end

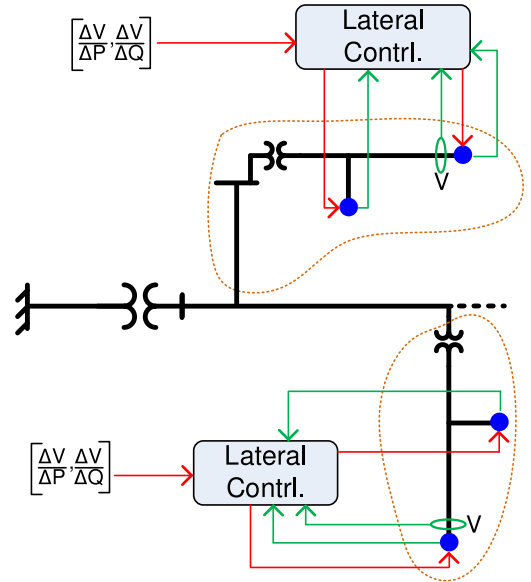Fig. 3. Active and power control based on sensitivity-based approach.

- If the voltage magnitude of the end node of a lateral is outside V_m^a/V_m^d, all the PVs on the lateral provide active power output information to the lateral controller, which is then used to find reactive power capability of a PV using $Q_m^c = \pm\sqrt{S_m^2 - P_m^2}$. Also, the sensor on the end node of the lateral provides the voltage information, which is then used by the controller to compute voltage increment $\left(\Delta V_m = Q_m^c \frac{\delta V_e}{\delta Q_m}\right)$ using the reactive power capability and sensitivity and sorted in a descending order.
- The difference of measured voltage magnitude at the end

node of a lateral and the minimum/maximum allowed limits ($\mathbf{V^{min}}$/$\mathbf{V^{max}}$) is calculated, i.e., $\mathbf{\Delta V_{e}^{Rq}}$. Then, the first $\mathbf{R}$ sorted reactive capability information that is sufficient to bring the voltage magnitude within the limits are selected, and dispatch signals are sent to the corresponding inverter controllers.

- If the reactive power capability of the inverters are not enough in maintaining the voltage, then we apply APC based on $\frac{\delta \mathbf{V_e}}{\delta \mathbf{P_m}}$ to compensate the remaining voltage difference. For fairness across PVs, we propose to curtail PV active power equally from all inverters using average sensitivity values.

Algorithm 2: Sensitivity-based Method of Control

---

while t < T do
 Run Power Flow
 while l < L do
  sort $\mathbf{\Delta V_{m,t} = Q_{m,t}^{c}\, \frac{\delta V_{e,t}}{\delta Q_{m,t}}}$
  if $\mathbf{V_{e,t} > V_{e}^{d}}$ **then**
   $\mathbf{\Delta V_{e,t}^{Rq} = V_{e}^{d} - V_{e,t}}$
  end
  if $\mathbf{V_{e,t} < V_{e}^{a}}$ **then**
   $\mathbf{\Delta V_{e,t}^{Rq} = V_{e,t} - V_{e}^{a}}$
  end
  while r < R do
   if $\mathbf{\Delta V_{e,t}^{Rq} < 0}$ **then**
    $\mathbf{Q_{m,t} = Q_{m,t} + Q_{m,t}^{c}}$
    $\mathbf{\Delta V_{e,t}^{Rq} = \Delta V_{e,t}^{Rq} + \Delta V_{m,t}}$
   else if $\mathbf{\Delta V_{e,t}^{Rq} > 0}$ **then**
    $\mathbf{Q_{m,t} = Q_{m,t} - Q_{m,t}^{c}}$
    $\mathbf{\Delta V_{e,t}^{Rq} = \Delta V_{e,t}^{Rq} - \Delta V_{m,t}}$
   else
    break
   end
  end
  if $\mathbf{\Delta V_{e,t}^{Rq} > 0}$ **then**
   while m < M do
    $\mathbf{P_{m,t}^{cur} = \dfrac{\Delta V_{e,t}^{Rq}}{\frac{1}{M}\sum_{n}\frac{\delta V_{e,t}}{\delta P_{n,t}}}}$
   end
  end
 end
end

C. Proposed Approach: Power Flow Sensitivities based Droops as per IEEE-1547

The droops $\mathbf{Q(V)}$ as shown in Fig. 1 could be obtained systematically using the power flow sensitivities. Thus, the reactive power to voltage sensitivities obtained from (1) are used to derive the slopes of $\mathbf{Q(V)}$ droops as following,

$$\mathbf{\beta_m = \gamma_m = \frac{\delta Q_m}{\delta V_m}} \tag{2}$$

The droop settings $\mathbf{Q(V)}$ obtained are sent to the inverter controllers at regular time interval, and then the local
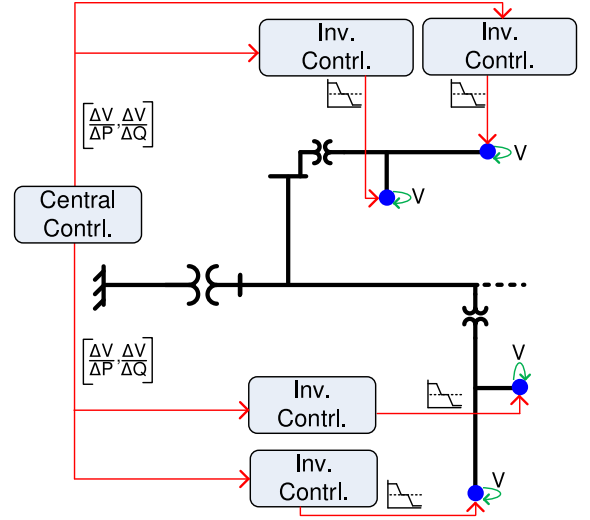

Fig. 4. Control based on droops obtained from power flow sensitivities.

controllers manage the reactive power output of each inverters as shown in Fig. 4. In reactive power priority mode, curtailment of active power may become necessary as in the method in Section III.A. To check whether active power curtailment is required or not, $\mathbf{P_m^2 + Q_m^2}$ is compared to squared of the inverter's apparent power rating $\mathbf{S_m^2}$. If the latter is smaller, then active power is curtailed. The algorithm of reactive power control and APC is similar to one in Algorithm 1.

D. Optimal Power Flow (OPF) based Control

For the centralized approach, OPF model can be solved to minimize APC utilizing inverters' reactive power capability, while maintaining operating limits and power balance equations. The control schema for an OPF-based method for voltage control is provided in Fig. 5. A generic OPF model for this purpose can be formulated as,

$$\text{Min:} \quad \mathbf{E^{cur} = \sum_{m,t} P_{m,t}^{cur}\, \Delta t} \tag{3}$$

subject to:

$$\mathbf{I_{j,t} = \sum_{k \in N} Y_{j,k}\, V_{k,t} \quad \forall\, j, t} \tag{4}$$

$$\mathbf{P_{j,t} - P_{j,t}^{cur} - P_{j,t}^{L} = Real\left(V_{j,t}\, I_{j,t}^{*}\right) \quad \forall\, j, t} \tag{5}$$

$$\mathbf{Q_{j,t} - Q_{j,t}^{L} = Imag\left(V_{j,t}\, I_{j,t}^{*}\right) \quad \forall\, j, t} \tag{6}$$

$$\mathbf{V^{min} \leq |V_{m,t}| \leq V^{max} \quad \forall\, m, t} \tag{7}$$

$$\mathbf{Q_{m,t} \leq \sqrt{S_m^2 - \left(P_{m,t} - P_{m,t}^{cur}\right)^2} \quad \forall\, m, t} \tag{8}$$

$$\mathbf{Q_{m,t} \geq -\sqrt{S_m^2 - \left(P_{m,t} - P_{m,t}^{cur}\right)^2} \quad \forall\, m, t} \tag{9}$$

In the above formulation, (3) represents energy curtailment of PVs, (4) represents current injection equations at each node, (5) represents load/PV active power model, (6) represents load/PV reactive power model, (7) represents limits on the

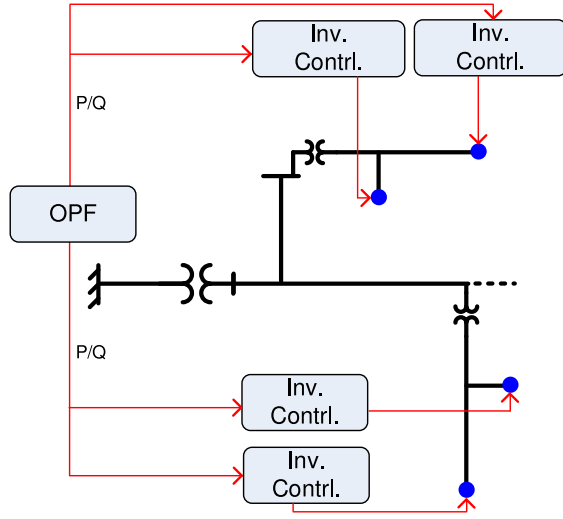voltage magnitude, (8) and (9) represent lower and upper bound on the reactive power of PVs.

Fig. 5. Inverter Control based on OPF solution.

IV. Numerical Simulations

This section provides details of performance studies of control based on the IEEE-1547 with arbitrary slopes, sensitivity-based method, IEEE-1547 with sensitivity-based droop settings, and OPF-based method in terms of voltage profile and power/energy curtailment.

A. Test System and Setup

Baran and Wu system [27] modified to a 730-node feeder as used in [28] (Fig. 6) was adopted for the studies with 70% and 100% PV penetration levels (by the number of LV nodes). These correspond to 306 and 436 number of inverters, respectively. Each inverter is rated 8 kW. We considered V^L=0.88 p.u., V^U=1.1 p.u., V^{min}=0.95 p.u., and V^{max}=1.05 p.u.
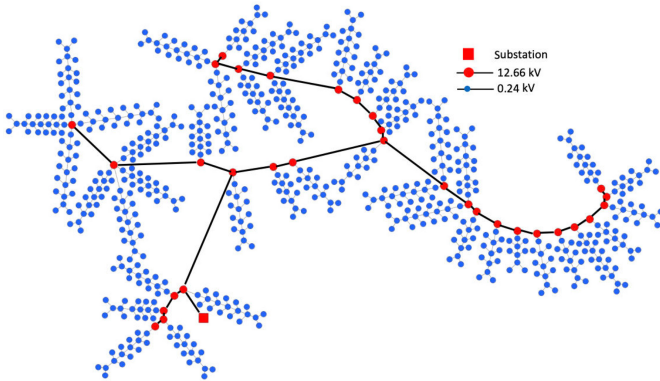

Fig. 6. 730-node MV/LV feeder used for the case studies [28].

Load profiles are similar to that used in [11] and represents realistic data. Fig. 7 shows net active and reactive power loads with 1-minute resolution for a typical day. We used two PV profiles as shown in Fig. 8: one corresponds to a sunny day (PV-1) and the second profile corresponds to a cloudy day (PV-2). We used Newton-Raphson based method in MATLAB

to perform daily load flow simulations on 1-minute resolution for the distributed approaches. For OPF-based approach, we modelled using GAMS and solved using KNITRO solver.
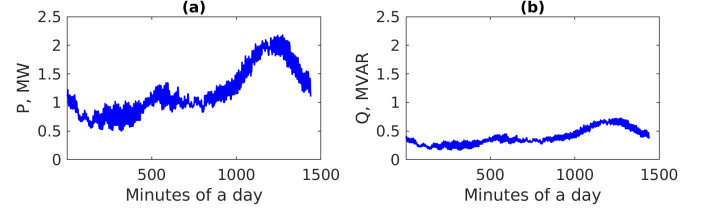

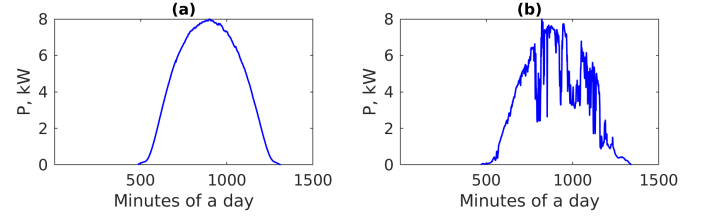Fig. 7. Total loads: a) active load profile, b) reactive load profile.

Fig. 8. PV profiles: a) PV-1 (sunny day), b) PV-2 (cloudy day).

B. IEEE-1547 with Arbitrary Droop Settings

IEEE-1547 prescribes range for the voltage break points for the $Q(V)$ curve in Fig. 1 [10]. Thus, we created random droop settings by arbitrarily choosing V^a, V^b, V^c, and V^d within the range prescribed in [10] for each inverter. Then, we performed a series of daily simulations with 1-minute time resolution, and the voltage profiles (maximum voltage on the feeder) obtained from the base case (assuming no control over PVs) simulation and with control of PVs are compared in Fig. 9. The base case shows that the feeder has over-voltage issues during day time when PV output is high.
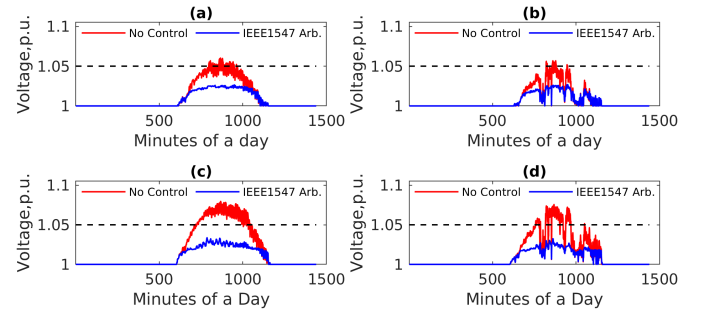

Fig. 9. Max. voltage with base case vs. IEEE-1547 with arbitrary droops: a) 70% PV, PV-1, b) 70% PV, PV-2, c) 100% PV, PV-1, and d) 100% PV, PV-2.

With droop settings as per the IEEE-1547 guidelines, though the settings are randomized for each inverter, no over-voltage issues were observed. However, It can be seen that the maximum voltage with inverter control is significantly below the maximum allowed limit of 1.05 p.u., which signifies that the droop settings are overly designed and could have caused higher APC and/or higher reactive power output from the PVs. APC of PVs are illustrated in Fig. 10. Non-zero APC means that the reactive power capability of inverters is not sufficient

to mitigate over-voltage issues, thus active power curtailment becomes necessary. It can be seen from Fig. 10 that with higher PV penetration, the controller needs to curtail higher power from PVs in order to maintain the feeder voltage profile.
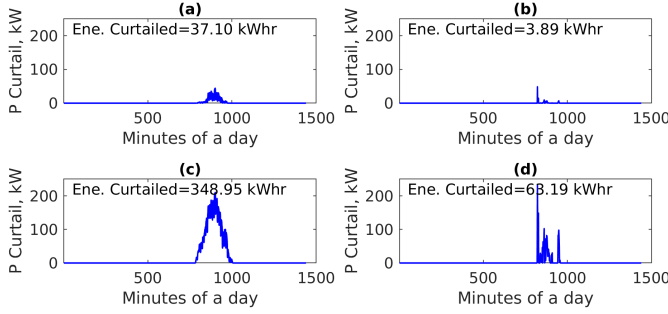

Fig. 10. APC obtained from the IEEE-1547 with arbitrary droop settings: a) 70% PV, PV-1, b) 70% PV, PV-2, c) 100% PV, PV-1, and d) 100% PV, PV-2.

C. Sensitivity-based Approach

The simulation results of sensitivity based method are plotted together with the base case results in Fig. 11. It can be observed that with sensitivity-based method, over-voltage problems can be generally solved. However, there are very few instances where over-voltage still persists. The over-voltage cases are shown in the insets of Fig. 11, and are very close to upper limit of 1.05 p.u. The over-voltage cases are observed around the time when PV outputs are at their maximum. Since, we assumed not all node voltage measurements are available at the lateral level controller, the proposed approach can lead to instances of over-voltage. Another reason could be attributed
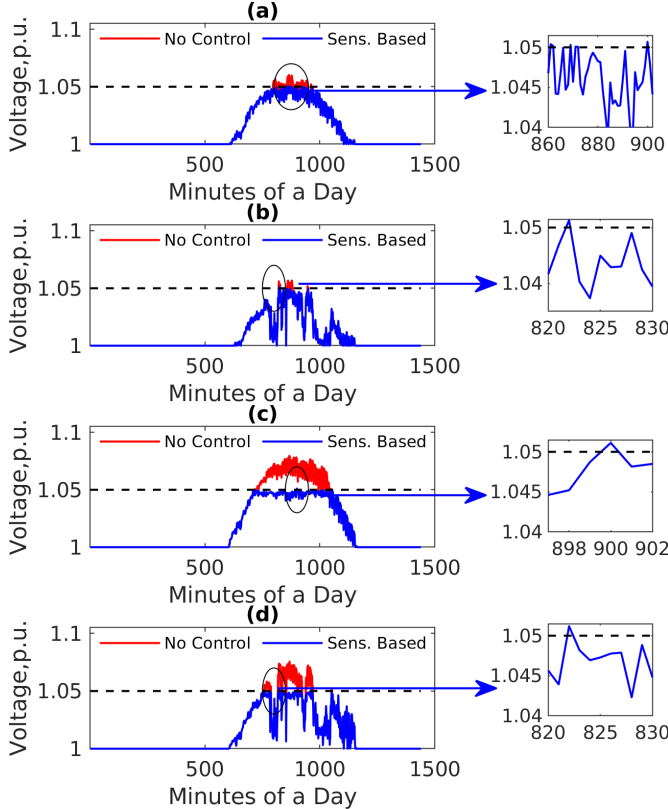
to the constant sensitivity, which are computed offline, and leads to error due to approximation.

We illustrate APC obtained from the sensitivity-based in Fig. 12. Compared to the IEEE-1547 droop based approach, APC using sensitivity-based method is less for 70% PV penetration level and more for 100% PV penetration level. As the penetration level increases, more power/energy needs to be curtailed.
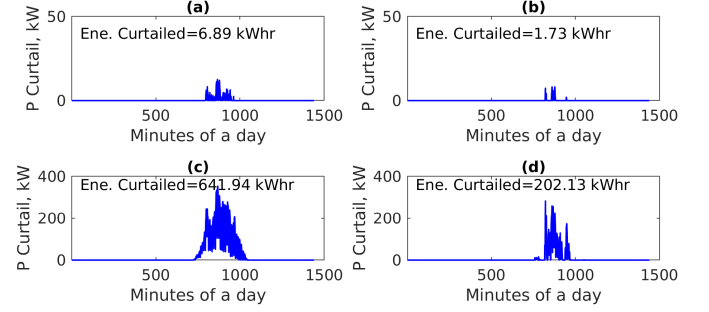

Fig. 12. APC from sensitivity-based method: a) 70% PV, PV-1, b) 70% PV, PV-2, c) 100% PV, PV-1, and d) 100% PV, PV-2.

D. IEEE-1547 with Power Flow Sensitivities

Simulation results of IEEE-1547 based method using sensitivities are illustrated together with base case results in Fig. 13. It is observed that using sensitivity-based $Q(V)$ droops perform very similar to arbitrarily chosen droops as per the IEEE-1547 (as discussed in the Section II.B). Fig. 14 shows APC obtained from the droop settings based on power flow sensitivities.
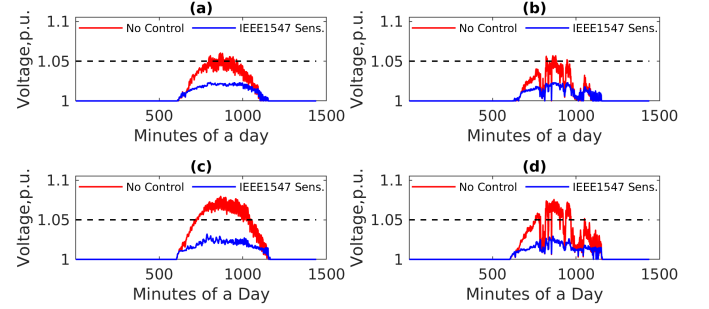

Fig. 13. Max. voltage with base case vs. IEEE-1547 droops obtained from the sensitivities: a) 70% PV, PV-1, b) 70% PV, PV-2, c) 100% PV, PV-1, and d) 100% PV, PV-2.

Fig. 11. Max. voltage with base case vs. sensitivity-based method: a) 70% PV, PV-1, b) 70% PV, PV-2, c) 100% PV, PV-1, and d) 100% PV, PV-2.
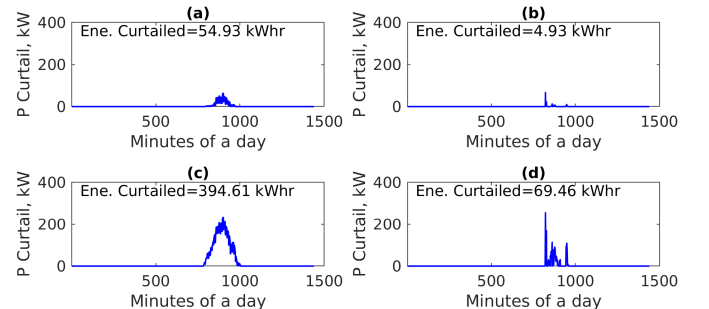

Fig. 14. APC from IEEE-1547 droops obtained from the sensitivities: a) 70% PV, PV-1, b) 70% PV, PV-2, c) 100% PV, PV-1, and d) 100% PV, PV-2.

E. OPF-based Approach

The maximum feeder voltage profile obtained using OPF-based method is compared with the base case in Fig. 15. From the case studies, it can be seen that the OPF-based approach can completely eliminate the over-voltage issues. APC obtained from OPF-based method is shown in Fig. 16.
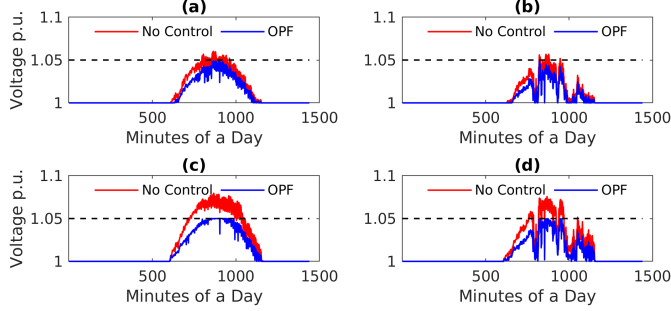

Fig. 15. Max. voltage with base case vs. OPF-based method: a) 70% PV, PV-1 b) 70% PV, PV-2 c) 100% PV, PV-1, and d) 100% PV, PV-2.
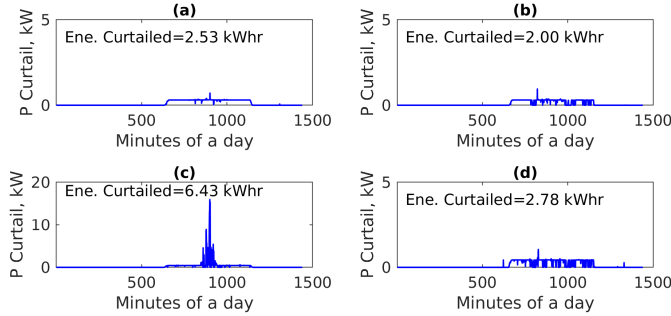

Fig. 16. APC from OPF-based method: a) 70% PV, PV-1 , b) 70% PV, PV-2, c) 100% PV, PV-1, and d) 100% PV, PV-2.

F. Comparative Analysis

To compare performances of all the methods, we define a voltage performance index (VPI) based on voltage profile compared to maximum allowed upper bound of 1.05 p.u. Let's consider ω represents the window of time in which over-voltage occurred for the base case simulation. Then, VPI for each method and PV penetration scenario is obtained as: $\text{VPI} = \sum_{j,t \in \omega} (V_{j,t} - 1.05)$. A lower value of VPI is desired and a value of zero means a perfect voltage performance. Since the main objective of the controllers would be to keep the voltage below 1.05 p.u; a voltage profile significantly below 1.05 p.u. may suggest unnecessary use of reactive power or APC of PVs. Therefore, an ideal control method would try to keep the voltage just below 1.05 p.u. but as close to 1.05 p.u. as possible. Table I shows summary of VPI in p.u. The base case shows positive VPI which means the over-voltage issue exists on the feeder. From the results, it can be observed that the sensitivity-based method yields minimum VPI even though the sensitivity-based approach may not completely mitigate the over-voltage issue. It is interesting to note that the VPI for sensitivity-based method is even better than the OPF-based method, and this could possibly because of local optimal solutions of OPF-based approach given the OPF model is non-convex in nature. The droop settings (as per the IEEE-1547),

whether that be arbitrary slopes or slopes based on sensitivity-based approach, yield large negative VPI values. This means these methods unnecessarily over corrects the over-voltage issue as the voltage profile is significantly below 1.05 p.u. (see Fig. 9 and Fig. 13).

TABLE I
COMPARISON OF VOLTAGE PERFORMANCE INDEX FOR THE VARIOUS METHODS.

PV Profile	PV-1		PV-2	
PV Level	70%	100%	70%	100%
Base Case	0.35	5.22	0.09	2.02
IEEE-1547 Arb.	-2.41	-7.61	-0.65	-3.91
Sensitivity-based	-0.38	-1.09	-0.13	-0.50
IEEE-1547 Sens.	-2.71	-8.49	-0.73	-4.28
OPF-based	-0.54	-1.59	-0.25	-1.28

The comparison of energy curtailment obtained from all methods with respect to OPF-based (in the multiples of energy curtailment obtained from OPF) is given in Table II. The energy curtailment of OPF-based method is generally minimum. However, there could be cases when the OPF solution is local optimal and hence the energy curtailment obtained from OPF may become larger than other methods (see sensitivity-based method for 70% PV penetration with the second PV profile). Energy curtailment obtained from both IEEE-1547 droop-based methods are similar. Though the voltage performance index of sensitivity-based method is better, the sensitivity-based method often leads to larger power/energy curtailments compared to the IEEE-1547 droop-based methods.

TABLE II
COMPARISON OF ENERGY CURTAILMENT FOR THE VARIOUS METHODS (IN THE MULTIPLES OF ENERGY CURTAILMENT OBTAINED FROM OPF).

PV Profile	PV-1		PV-2	
PV Level	70%	100%	70%	100%
IEEE-1547 Arb.	14.64	54.27	1.95	24.53
Sensitivity-based	2.72	99.83	0.87	72.71
IEEE-1547 Sens.	21.72	61.37	2.47	24.99

G. Monte Carlo Simulation

We also performed Monte Carlo simulation by varying PV penetration level to evaluate the average performance of the four approaches. For each penetration level (randomized 25%, 50%, 75% and 100% by varying PV location) 1,000 different simulations were run for base case, IEEE-1547 with arbitrary settings, sensitivity based method, IEEE-1547 with sensitivity based settings and OPF-based method. The minimum and maximum of the maximum feeder voltage obtained from the 1,000 runs are shown in Fig. 17 along with the upper voltage bound of 1.05 p.u. The feeder exhibits over-voltage issues above 50% penetration level without any control. IEEE-1547 over-voltage with arbitrary settings, IEEE-1547 with sensitivity based settings and OPF-based approaches are able to solve over-voltage issue for any penetration level. On the other hand, sensitivity-based method may not mitigate over-voltage issue completely as slight over-voltage above 1.05 p.u are observed occasionally.
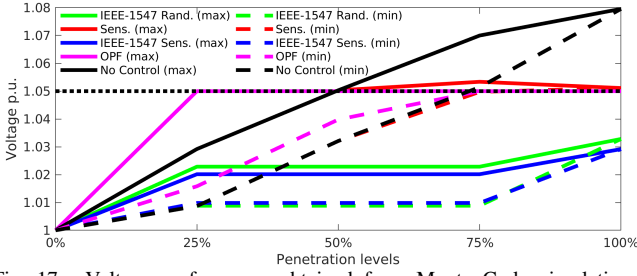
Fig. 17. Voltage performance obtained from Monte Carlo simulation by varying PV penetration level.

V. Conclusion

This work developed methods to locally control active/reactive power of smart inverters to regulate voltage profile on distribution feeders. First, a nodal sensitivity-based approach is adopted, and then combined with $\mathbf{Q(V)}$ droops as per the IEEE-1547 standard. Then, the performance is compared with arbitrary $\mathbf{Q(V)}$ droop settings and an OPF-based approach using a 730-node MV/LV with hundreds of PV inverters. The case studies demonstrate that the droop settings as per the IEEE-1547 can effectively mitigate overvoltage issues. However, the droop settings tend to be overly designed that cause unnecessarily higher correction of over-voltage issues as the resulting voltage profiles become significantly below the allowed voltage upper bounds. A sensitivity-based approach, though not fully able to solve the over-voltage problems, provides the best voltage performance index to mitigate the over-voltage issues by lowering the over-voltage magnitudes in the close vicinity of upper bounds. Given the communication need for centralized OPF-based method and despite non-optimal active power curtailment, the local droop-based approaches could still be alternatives to regulate voltage on distribution feeders with high penetration of PVs. As the penetration of smart inverter increases, and communication infrastructure becomes readily available, a centralized OPF-based control scheme could also become viable.

References

[1] F. Katiraei and J. R. Aguero, "Solar PV integration challenges," *IEEE Power and Energy Magazine*, vol. 9, no. 3, pp. 62–71, May 2011.

[2] Y. Liu, J. Bebic, B. Kroposki, J. de Bedout, and W. Ren, "Distribution system voltage performance analysis for high-penetration PV," in *2008 IEEE Energy 2030 Conference*, Nov 2008, pp. 1–8.

[3] A. Chidurala, T. K. Saha, and N. Mithulananthan, "Harmonic impact of high penetration photovoltaic system on unbalanced distribution networks–learning from an urban photovoltaic network," *IET Renewable Power Generation*, vol. 10, no. 4, pp. 485–494, 2016.

[4] R. Tonkoski, L. A. Lopes, and T. H. El-Fouly, "Coordinated active power curtailment of grid connected pv inverters for overvoltage prevention," *IEEE Transactions on Sustainable Energy*, vol. 2, no. 2, pp. 139–147, 2011.

[5] Y. Ueda, K. Kurokawa, T. Tanabe, K. Kitamura, and H. Sugihara, "Analysis results of output power loss due to the grid voltage rise in grid-connected photovoltaic power generation systems," *IEEE Transactions on Industrial Electronics*, vol. 55, no. 7, pp. 2744–2751, July 2008.

[6] D. McPhail, B. Croker, and B. Harvey, "A study of solar PV saturation limits for representative low voltage networks," in *Proc. Australasian Universities Power Engineering Conference (AUPEC)*, 2016, pp. 1–6.

[7] I. Roytelman, B. K. Wee, and R. L. Lugtu, "Volt/var control algorithm for modern distribution management system," *IEEE Transactions on Power Systems*, vol. 10, no. 3, pp. 1454–1460, Aug 1995.

[8] S. R. Abate, T. E. McDermott, M. Rylander, and J. Smith, "Smart inverter settings for improving distribution feeder performance," in *Proc. IEEE Power Energy Society General Meeting*, 2015, pp. 1–5.

[9] F. Ding, A. Nagarajan, S. Chakraborty, M. Baggu, A. Nguyen, S. Walinga, M. McCarty, and F. Bell, "Photovoltaic impact assessment of smart inverter volt-var control on distribution system conservation voltage reduction and power quality," National Renewable Energy Lab. (NREL), Golden, CO (United States), Tech. Rep., 2016.

[10] "IEEE standard for interconnection and interoperability of distributed energy resources with associated electric power systems interfaces," *IEEE Std 1547-2018 (Revision of IEEE Std 1547-2003)*, pp. 1–138, 2018.

[11] S. Paudyal, B. P. Bhattarai, R. Tonkoski, S. Dahal, and O. Ceylan, "Comparative study of active power curtailment methods of pvs for preventing overvoltage on distribution feeders," in *Proc. IEEE Power Energy Society General Meeting*, 2018, pp. 1–5.

[12] C.-H. Lin, W.-L. Hsieh, C.-S. Chen, C.-T. Hsu, and T.-T. Ku, "Optimization of photovoltaic penetration in distribution systems considering annual duration curve of solar irradiation," *IEEE Transactions on Power Systems*, vol. 27, no. 2, pp. 1090–1097, 2012.

[13] S. Ghosh, S. Rahman, and M. Pipattanasomporn, "Distribution voltage regulation through active power curtailment with pv inverters and solar generation forecasts," *IEEE Transactions on Sustainable Energy*, vol. 8, no. 1, pp. 13–22, Jan 2017.

[14] A. Molina-García, R. A. Mastromauro, T. García-Sánchez, S. Pugliese, M. Liserre, and S. Stasi, "Reactive power flow control for pv inverters voltage support in lv distribution networks," *IEEE Transactions on Smart Grid*, vol. 8, no. 1, pp. 447–456, Jan 2017.

[15] G. Mokhtari, A. Ghosh, G. Nourbakhsh, and G. Ledwich, "Smart robust resources control in lv network to deal with voltage rise issue," *IEEE Transactions on Sustainable Energy*, vol. 4, no. 4, pp. 1043–1050, Oct 2013.

[16] O. Gagrica, P. H. Nguyen, W. L. Kling, and T. Uhl, "Microinverter curtailment strategy for increasing photovoltaic penetration in low-voltage networks," *IEEE Transactions on Sustainable Energy*, vol. 6, no. 2, pp. 369–379, April 2015.

[17] T. T. Ku, C. H. Lin, C. S. Chen, C. T. Hsu, W. L. Hsieh, and S. C. Hsieh, "Coordination of pv inverters to mitigate voltage violation for load transfer between distribution feeders with high penetration of pv installation," *IEEE Transactions on Industry Applications*, vol. 52, no. 2, pp. 1167–1174, March 2016.

[18] E. Demirok, P. C. Gonzalez, K. H. Frederiksen, D. Sera, P. Rodriguez, and R. Teodorescu, "Local reactive power control methods for overvoltage prevention of distributed solar inverters in low-voltage grids," *IEEE Journal of Photovoltaics*, vol. 1, no. 2, pp. 174–182, 2011.

[19] M. E. Baran and I. M. El-Markabi, "A multiagent-based dispatching scheme for distributed generators for voltage support on distribution feeders," *IEEE Transactions on Power Systems*, vol. 22, no. 1, pp. 52–59, 2007.

[20] S. Weckx, C. Gonzalez, and J. Driesen, "Combined central and local active and reactive power control of pv inverters," *IEEE Transactions on Sustainable Energy*, vol. 5, no. 3, pp. 776–784, 2014.

[21] X. Su, M. A. Masoum, and P. J. Wolfs, "Optimal pv inverter reactive power control and real power curtailment to improve performance of unbalanced four-wire lv distribution networks," *IEEE Transactions on Sustainable Energy*, vol. 5, no. 3, pp. 967–977, 2014.

[22] J. Zhao, A. Golbazi, C. Wang, Y. Wang, L. Xu, and J. Lu, "Optimal and fair real power capping method for voltage regulation in distribution networks with high pv penetration," in *Proc. IEEE Power Energy Society General Meeting*, July 2015, pp. 1–5.

[23] G. Cavraro, S. Bolognani, R. Carli, and S. Zampieri, "The value of communication in the voltage regulation problem," in *2016 IEEE 55th Conference on Decision and Control (CDC)*, Dec 2016, pp. 5781–5786.

[24] P. Jahangiri and D. C. Aliprantis, "Distributed volt/var control by pv inverters," *IEEE Transactions on power systems*, vol. 28, no. 3, pp. 3429–3439, 2013.

[25] P. D. F. Ferreira, P. M. S. Carvalho, L. A. F. M. Ferreira, and M. D. Ilic, "Distributed energy resources integration challenges in low-voltage networks: Voltage control limitations and risk of cascading," *IEEE Transactions on Sustainable Energy*, vol. 4, no. 1, pp. 82–88, Jan 2013.

[26] F. Olivier, P. Aristidou, D. Ernst, and T. V. Cutsem, "Active management of low-voltage networks for mitigating overvoltages due to photovoltaic units," *IEEE Transactions on Smart Grid*, vol. 7, no. 2, pp. 926–936, March 2016.

[27] M. E. Baran and F. F. Wu, "Network reconfiguration in distribution systems for loss reduction and load balancing," *IEEE Transactions on Power Delivery*, vol. 4, no. 2, pp. 1401–1407, Apr. 1989.

[28] H. K. Vemprala, M. A. I. Khan, and S. Paudyal, "Open-source polyphase distribution system power flow analysis tool (DxFlow)," in *Proc. IEEE Int. Conference on Electro Information Technology*, 2019, pp. 1–6.